Supplementary Information for:

Degradation Kinetics and Secondary Organic Aerosol Formation from Eugenol by Hydroxyl Radicals

Changgeng Liu[1,2], Yongchun Liu[1,3,4,a,*], Tianzeng Chen[1,4], Jun Liu[1,4], Hong He[1,3,4,*]

[1]State Key Joint Laboratory of Environment Simulation and Pollution Control, Research Center for Eco-Environmental Sciences, Chinese Academy of Sciences, Beijing 100085, China

[2]School of Biological and Chemical Engineering, Panzhihua University, Panzhihua 617000, China

[3]Center for Excellence in Regional Atmospheric Environment, Institute of Urban Environment, Chinese Academy of Sciences, Xiamen 361021, China

[4]University of Chinese Academy of Sciences, Beijing 100049, China

[a]Currently at: Beijing Advanced Innovation Center for Soft Matter Science and Engineering, Beijing University of Chemical Technology, Beijing 100029, China

Correspondence to: Yongchun Liu (liuyc@buct.edu.cn) and Hong He (honghe@rcees.ac.cn)

Experimental details

OH radical reactions were performed in an oxidation flow reactor (OFR) consisting of two electro-polished stainless steel cylinders, i.e., the static mixing tube (29.3 cm (length)) and the reaction chamber (7.3 cm (inner diameter) × 25 cm (length)). Before entering into the reaction chamber, gas-phase species were mixed sufficiently in the mixing tube. Fluid dynamics simulations of mixing tube confirmed that gas-phase species were well mixed with a uniform initial velocity profile. The average reaction time of OH with eugenol was 26.7 s calculated from the illuminated volume (0.89 L) and the total flow rate (2 L min^{-1}). The temperature of the reactor was maintained at 301 K by circulating water through the outer jacket of the OFR.

Liquid pure eugenol placed in a brown bubbler was gently heated and the carrier gas (zero air) brought gas-phase eugenol into the OFR. The concentrations of gas-phase eugenol in the OFR were controlled by the flow rate of carrier gas. Similarly, gas-phase reference compound (*m*-xylene and 1,3,5-trimethylbenzene) was also introduced into the OFR via a brown bubbler without heating. The concentrations of gas-phase species were determined by a commercial high-resolution proton-transfer reaction time-of-flight mass spectrometer (HR-PTR-QiToF-MS) (Ionicon Analytik GmbH). The concentration of eugenol was calibrated by a commerial permeation tube (VICI AG INTERNATIONAL Valco Instruments Co., Inc.). The toolkit Squirrel 1.16H was used to analyze the mass concentrations of sulfate, nitrate, and organics, measured by an Aerodyne high-resolution time-of-flight aerosol mass spectrometer (HR-ToF-AMS).

NO_2 concentration was determined by a NO_x analyzer (Model 42i-TL, Thermo Fisher Scientific Inc.).

In this work, control experiments showed that the concentrations of eugenol and reference compounds were not influenced by O_3. These results were mainly resulted from the short reaction time in the OFR and the low rate constants of O_3 with methoxyphenols (~10^{-19} cm^3 $molecule^{-1}$ s^{-1}) (El Zein et al., 2015) and reference compounds (~10^{-21} cm^3 $molecule^{-1}$ s^{-1}) (Atkinson et al., 1982; Yu et al., 2012). The concentrations of OH radicals were measured using SO_2 as the reference compound in a manner described previously (Lambe et al., 2015; Zhang et al., 2017). Approximately 200 ppbv SO_2 was introduced into the OFR by mass flow controller (MFC). Control experiments showed that SO_2 concentration was not affected individually by vapor H_2O, O_3, and 254 nm UV light. OH exposure ([OH]t) was determined from the measured fractional loss of SO_2, $[SO_2]/[SO_2]_0$.

$$[OH]t = -\frac{1}{k_{SO_2}} \ln \frac{[SO_2]}{[SO_2]_0} \quad \text{(S1)}$$

where k_{SO_2} is the second-order rate consant of SO_2 with OH radicals at 298 K (9×10^{-13} cm^3 $molecule^{-1}$ s^{-1}) (Davis et al., 1979).

Eugenol (Sigma-Aldrich, 99%), 1,3,5-trimethylbenzene (Sigma-Aldrich, 99.8%), and *m*-xylene (Sigma-Aldrich, 99.5%) were used in the experiments as received. NO_2 (105 ppmv) and SO_2 (100 ppmv) were from Beijing Huayuan Gas Chemical Industry Co., Ltd.

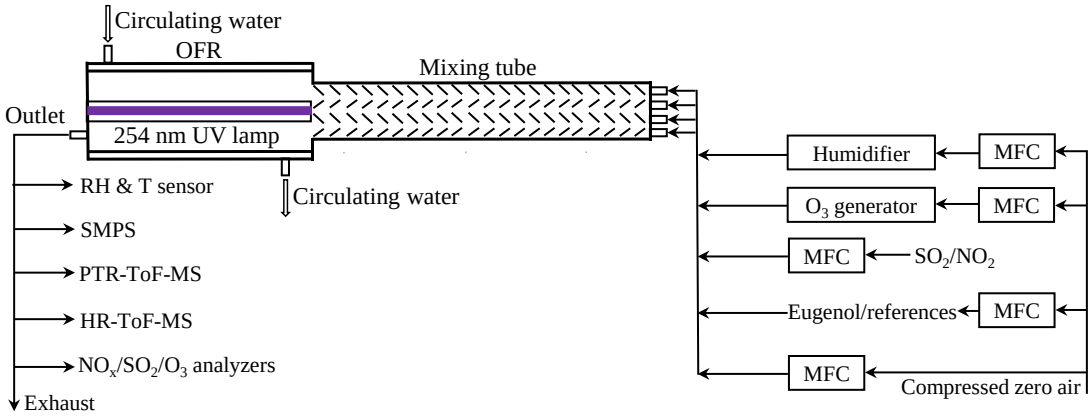

58

59 **Figure S1.** Experimental system used in this work.

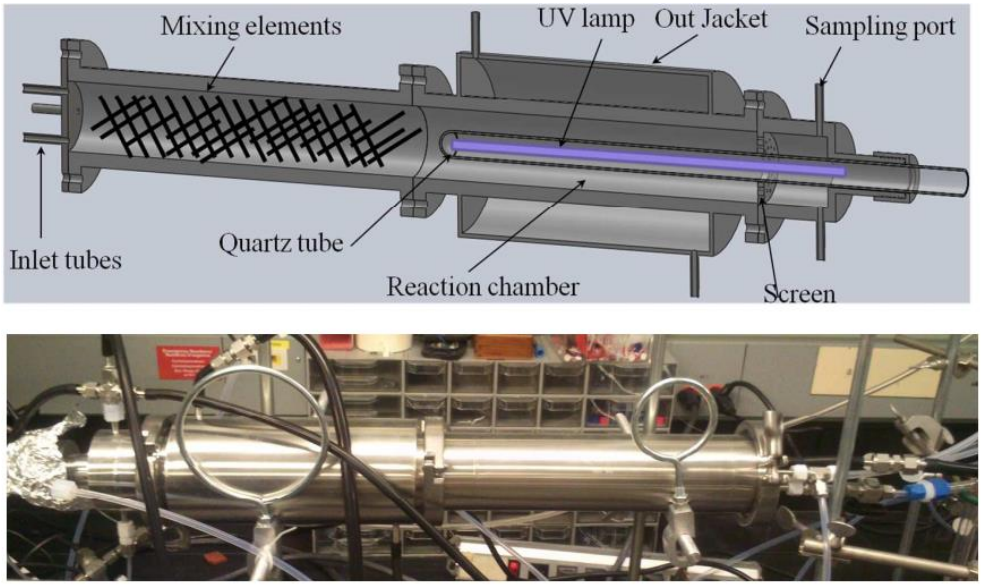

60

61 **Figure S2.** Detailed view of the Flow Oxidation Reactor and a photo of the reaction

62 system.

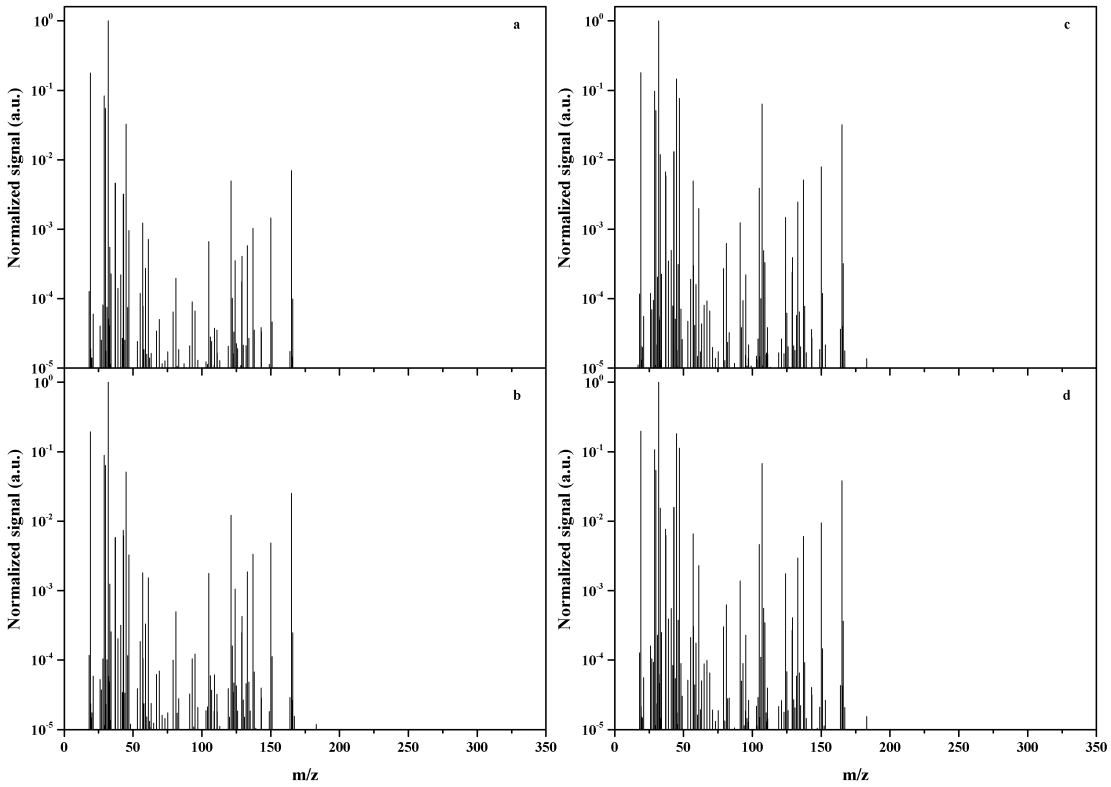

Figure S3. Normalized mass spectra of the gas mixtures of eugenol and 1,3,5-trimethylbenzene in the dark (a) and light (b), as well as eugenol and *m*-xylene in the dark (c) and light (d).

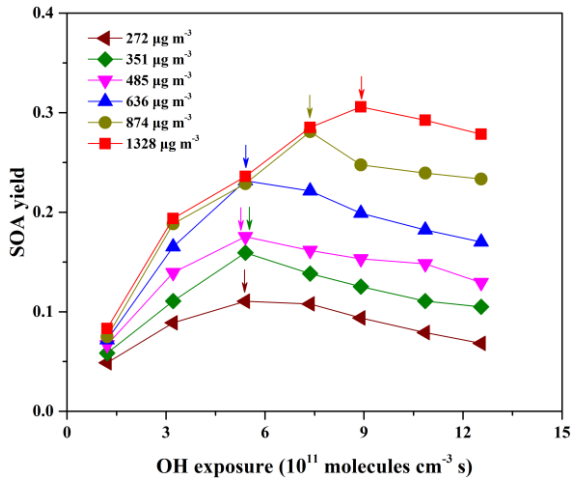

Figure S4. SOA yield vs. OH exposure for SOA formed from different eugenol concentrations.

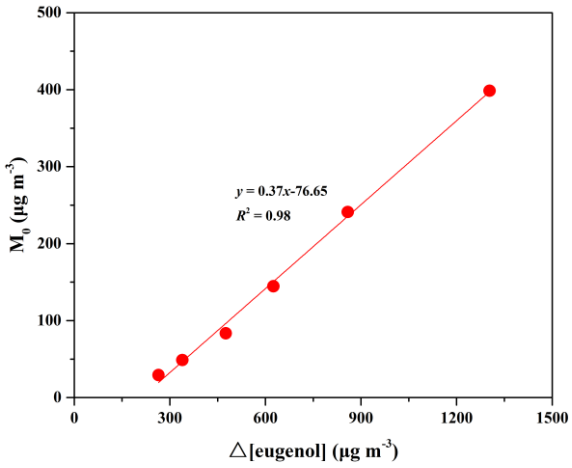

Figure S5. SOA mass concentration (M_0) vs. consumed eugenol concentration (△[eugenol]). Each data point represents a separate experiment.

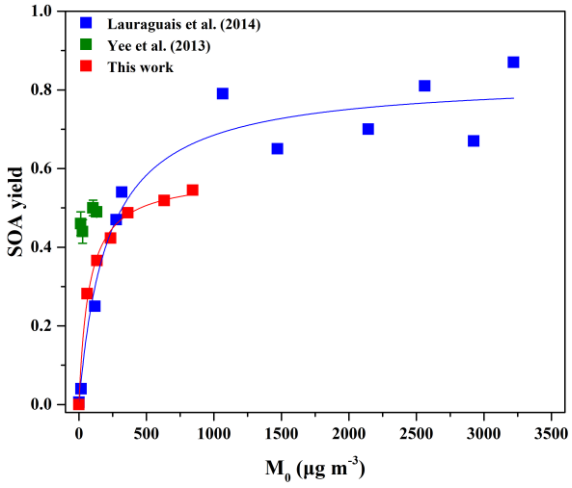

Figure S6. SOA yield as a function of SOA mass concentration (M_0) formed from the OH reactions at different guaiacol concentrations. The solid lines were fit to the experimental data using an one-product model. Values of α and $K_{om,i}$ used to generate the solid line are (0.58 ± 0.02) and (0.014 ± 0.001) in this work, and their values are (0.83 ± 0.04) and (0.005 ± 0.001) for the blue data from Lauraguais et al.(2014). The olive data are obtained from Yee et al. (2013).

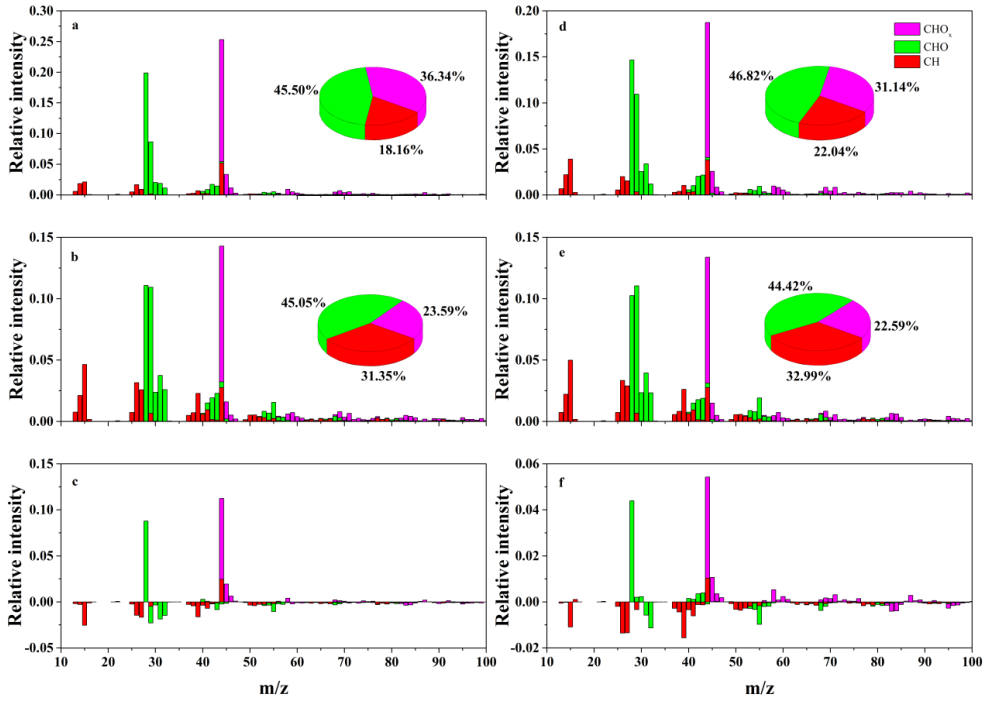

Figure S7. (a and d) Mass spectra of SOA at OH exposure of 12.55 × 10^{11} molecules s^{-1}. (b and e) Mass spectra of SOA at OH exposure of 1.21 × 10^{11} molecules s^{-1}. (c) Difference in mass spectra between (a) and (b). (f) Difference in mass spectra between (d) and (e). The data of (a-c) and (d-f) were taken from the aging processes of eugenol at two concentrations of 272 and 1328 μg m^{-3}, respectively.

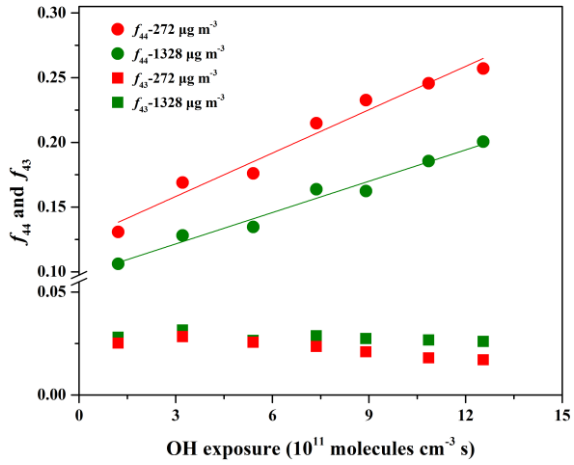

Figure S8. f_{44} and f_{43} vs. OH exposure for SOA formed at two eugenol concentrations (272 and 1328 μg m^{-3}).

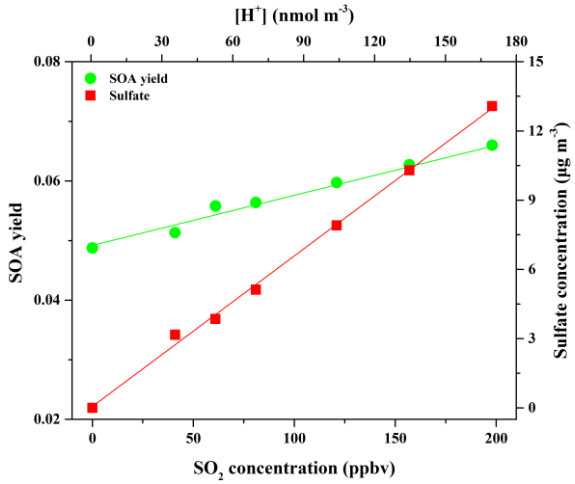

Figure S9. Effects of SO_2 concentration on SOA yield and sulfate formation in the reaction of eugneol with OH radicals at OH exposure and eugenol concentration of 1.21 $\times 10^{11}$ molecules cm^{-3} s and 264 μg m^{-3}, respectively. The in situ particle acidity was calculated as H^+ concentrations ($[H^+]$) according to the AIM-II model for $H-NH_4^+-SO_4^{2-}-NO_3^--H_2O$ system.

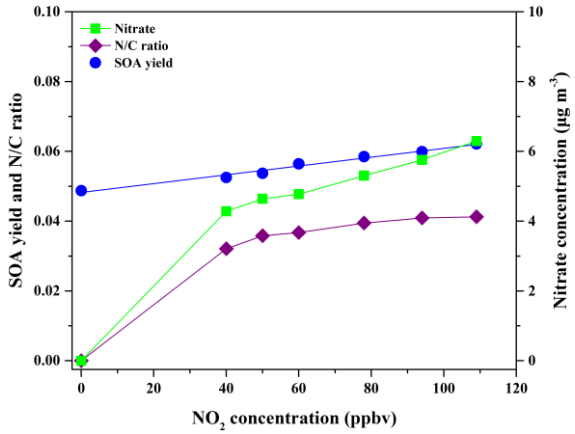

Figure S10. Evolution of SOA yield, nitrate formation, and N/C ratio as a function of NO_2 concentration at OH exposure and eugenol concentration of 1.21 $\times 10^{11}$ molecules cm^{-3} s and 268 μg m^{-3}, respectively.

References

Atkinson, R., Aschmann, S. M., Fitz, D. R., Winer, A. M., Pitts, J. N.: Rate constant for the gas-phase reactions of O_3 with selected organics at 296 K, Int. J. Chem. Kinet. 14, 13-18, doi: 10.1002/kin.550140103, 1982.

Davis, D.D., Ravishankara, A.R., Fischer, S.: SO_2 oxidation via the hydroxyl radical: Atmospheric fate of HSO_x radicals, Geophys. Res. Lett., 6, 113-116, doi: 10.1029/GL006i002p00113, 1979.

El Zein, A., Coeur, C., Obeid, E., Lauraguais, A., Fagniez, T.: Reaction kinetics of catechol (1,2-benzenediol) and guaiacol (2-methoxyphenol) with ozone, J. Phys. Chem. A 119, 6759-6765, doi: 10.1016/j.atmosenv.2013.11.074, 2015.

Lambe, A.T., Chhabra, P.S., Onasch, T.B., Brune, W.H., Hunter, J.F., Kroll, J.H., Cummings, M.J., Brogan, J.F., Parmar, Y., Worsnop, D.R., Kolb, C.E., Davidovits, P.: Effect of oxidant concentration, exposure time, and seed particles on secondary organic aerosol chemical composition and yield, Atmos. Chem. Phys., 15, 3063-3075, doi: 10.5194/acp-15-3063-2015, 2015.

Lauraguais, A., Coeur-Tourneur, C., Cassez, A., Deboudt, K., Fourmentin, M., Choel, M.: Atmospheric reactivity of hydroxyl radicals with guaiacol (2-methoxyphenol), a biomass burning emitted compound: Secondary organic aerosol formation and gas-phase oxidation products, Atmos. Environ., 86, 155-163, doi: 10.1016/j.atmosenv.2013.11.074, 2014.

Yee, L.D., Kautzman, K.E., Loza, C.L., Schilling, K.A., Coggon, M.M., Chhabra, P.S.,

Chan, M.N., Chan, A.W.H., Hersey, S.P., Crounse, J.D., Wennberg, P.O., Flagan, R.C., Seinfeld, J.H.: Secondary organic aerosol formation from biomass burning intermediates: Phenol and methoxyphenols, Atmos. Chem. Phys., 13, 8019-8043, doi: 10.5194/acp-13-8019-2013, 2013.

Yu, X., Yi, B., Wang, X., Chen, J.: Predicting reaction rate constants of ozone with organic compounds from radical structures, Atmos. Environ. 51, 124-130, doi: 10.1016/j.atmosenv.2012.01.037, 2012.

Zhang, X., Lambe, A. T., Upshur, M. A., Brooks, W. A., Be, A. G., Thomson, R. J., Geiger, F. M., Surratt, J. D., Zhang, Z.; Gold, A., Graf, S., Cubison, M. J., Groessl, M., Jayne, J. T., Worsnop, D. R., Canagaratna, M. R.: Highly oxygenated multifunctional compounds in alpha-pinene secondary organic aerosol, Environ. Sci. Technol. 51, 5932-5940, doi: 10.1021/acs.est.6b06588, 2017.